

Numerical simulation of turbulence interaction noise applied to a serrated airfoil

Cyril Polacsek[a)]
Vincent Clair[b)]
Thomas Le Garrec[c)]
Gabriel Reboul[d)]
National Aerospace Research Agency (Onera), MB 72, 92322 Châtillon, France

Turbulent wakes generated by turbofan blades and interacting with the outlet guide vanes are known to be mainly contributing to broadband noise emission of aero-engines at approach conditions. Analytical approaches, such as the well-known Amiet model can be adopted to estimate the noise generated by turbulent flows impacting thin airfoils, but they are limited by the flat-plate assumptions. The development of numerical methods allowing more complex geometries and realistic flows is required. The method described in the present paper, is based on a CAA code solving the nonlinear Euler equations. The upstream turbulence is synthesized from a stochastic model and injected into the computational domain through an adapted boundary condition. It is first validated in 2D and 3D against academic flat plate configurations by comparison with Amiet solutions (exact in such cases). Then, 3D computations are applied to simulate the effect of a passive treatment (leading edge serrations) aiming at reducing turbulence interaction noise of an isolated airfoil studied in the framework of European project FLOCON. First calculations on baseline conditions are shown to be able to reproduce the measured spectra and far-field directivities, and the acoustic performances of the serrations (3-4 dB PWL reduction) are fairly well assessed too.

1 INTRODUCTION

Turbulent wakes generated by turbofan blades and interacting with the outlet guide vanes are known to be mainly contributing to broadband noise emission of aero-engines at approach conditions. The prediction and the reduction of broadband noise component due to turbulent sources interactions are then highly required by engine manufacturers. As turbofan rotor-stator full 3D stage is out of reach of today computing capabilities, turbulent sources are generally

[a)] email: cyril.polacsek@onera.fr
[b)] email: vincent.clair@onera.fr
[c)] email: thomas.le_garrec@onera.fr
[d)] email: gabriel.reboul@onera.fr

studied through simplified configurations for which high-fidelity numerical simulations can be investigated, when analytical modeling is no longer possible. This was the motivation of two consecutive European projects PROBAND and FLOCON, respectively devoted to turbofan broadband noise prediction and reduction, by focusing on identified source mechanisms applied to generic cases such as rod-airfoil[1] or turbulence-airfoil[2] configurations. Passive treatments aiming at reducing turbulence interaction noise have been studied in FLOCON. A concept based on sinusoidal serrations (wavy edges) at the leading edge of a single airfoil has been investigated by Onera. Turbulence-airfoil interaction mechanism was studied using a turbulence grid located upstream of a NACA airfoil tested in ISVR (Institute of Sound and Vibration Research) anechoic open wind tunnel. High noise reductions have been obtained[3] for all studied flow speeds and prediction methods have been investigated to try to assess these results.

Analytical approaches, such as the well-known Amiet model[4] can be adopted to estimate the noise generated by turbulent flows impacting thin airfoils, but they are limited by the flat-plate assumptions. The development of numerical methods allowing more complex geometries and realistic flows is required. This is mandatory for example to study the serration effects on acoustics. Gust-airfoil interaction problem has been extensively investigated in numerous publications and more recently extended to turbulent source problem by means of different stochastic models to be coupled to the CAA. Lockard and Morris[5] solved the gust-airfoil interaction case for NACA 0006 and NACA 0012 using their Navier-Stokes code. Scott[6] provided benchmark solutions using the linearized Euler solver GUST3D for a linear vortical gust impinging on a Joukowski airfoil. Golubev et al.[7,8] performed a vast study on the gust-airfoil interaction, taking interest on high frequencies and high amplitude effects. Hixon et al.[9-11] also worked on this problem using the NASA code BASS. Then it was applied to a two-dimensional cascade and recently to a three-dimensional annular cascade.

Broadband calculations using turbulence stochastic models have been performed by Ewert[12] for slat noise predictions. The generation of the turbulent field is obtained by filtering white noise. Dieste & Gabard[13] also use this kind of stochastic model to simulate the turbulent wake / flat plate interaction. Salem-Said[14] interests in the interaction between a homogeneous turbulence with a flat plate cascade using LES and a Fourier-modes decomposition of a prescribed kinetic energy spectrum to synthesize the turbulent inflow.

In FLOCON project, two different numerical methods have been proposed by Onera to compute turbulence-airfoil interaction noise. Each method is aiming to simulate baseline and serrated airfoil cases and to be compared to the experimental results. The first method, developed by CERFACS is based on a RANS-LES chaining[15]. The second method, described in the present paper, is based on a CAA code solving the nonlinear Euler equations. In the two methods the upstream turbulence is synthesized from a stochastic model and injected into the computational domain through an adapted boundary condition. The CAA methodology and computation results are discussed in the paper.

2 METHODOLOGY

2.1 CAA code

The current calculations are performed with the Onera code sAbrinA.v0[16]. It solves the full Euler equations in the time domain, and applying a perturbation form that consists in a splitting of the conservative variables into a mean flow and a disturbance field. These equations are cast in generalized curvilinear coordinates to simulate flows around complex bodies. Such solving is conventionally conducted with the help of low-dissipative high-order finite differences (6th order

spatial derivatives and 10th order filters), and a 3rd order Runge-Kutta (RK3) time marching scheme. The code features multi-block structured grids and is parallelized using the MPI library.

To perform rotor-stator interaction CAA calculations, efficient computational boundary conditions are required to allow hydrodynamic perturbations to be imposed at the inflow boundary and both hydrodynamic and acoustic outgoing waves to exit the computational domain without reflection. For this purpose, Tam and Webb[17] inflow and outflow boundary conditions are applied. These conditions are very well suited to the present problem devoted to the injection of harmonic gusts from the inlet boundary of the CAA domain. The initial boundary conditions written using a spherical coordinate system can be adapted to a cylindrical one, more suited to the geometry when the span is long and periodicity conditions along spanwise direction are imposed in the CAA.

2.2 Synthetic turbulence model

The stochastic model presented here is inspired from Kraichnan theory[18]. It is based on a Fourier-modes decomposition of the incoming turbulent wake[14] modeled by a homogeneous isotropic turbulence (HIT) energy spectrum. In the present study, only the upwash velocity (component normal to the airfoil assimilated to a flat plate) is considered, as is done in Amiet theory[4]. Moreover, the parallel gusts are known to mainly contribute to the wake-airfoil acoustic response as soon as the span in large enough (practically beyond 3 chords) and when focusing to the 90° observer radiation in the centered plane normal to the span. Thus the modes can be restricted to axial wave numbers, which allows for drastically reducing the size and thus the CPU cost of the computations. The modes amplitudes are fitted by a Von Karman energy spectrum, defined by two parameters: the turbulence intensity, T_I, and the integral length scale, Λ.
Following the approach of Casper and Farassat[19], 3D calculations are performed using a two-wavenumber spectrum, $\Phi_{ww}\left(k_x,k_y\right)$, corresponding to the integration of the three-dimensional energy spectrum over the transverse wake number (k_z). Thus, the incoming upwash turbulent-like velocity field can be written as:

$$w_{upwash}\left(x,y,t\right)=\sum_{j=-N_y}^{N_y}\sum_{i=1}^{N_x}2\sqrt{\Phi_{ww}\left(k_{x,i},k_{y,j}\right)\Delta k_x\Delta k_y}\cos\left(\omega t-k_{x,i}x-k_{y,j}y+\varphi_{i,j}\right) \qquad (1)$$

The unsteady disturbance field is assumed to be convected through a uniform mean flow in the convection direction (Taylor's frozen turbulence hypothesis), so that the pulsation ω is related to the streamwise wavenumber $k_c = k_x$ by $\omega = k_c U_c$. $\varphi_{i,j}$ is a random phase associated to the (i,j) mode and chosen between 0 and 2π. When considering a realistic RANS mean flow in the CAA, the convection speed of the frozen turbulence in set equal to the undisturbed upstream flow. The synthetic turbulent field so obtained is inherently divergence-free, which prevents from creating any additional sound sources.

2.3 Acoustic radiation

Although the acoustic response of the airfoil can be directly provided by the Euler computation, far-field radiation is practically obtained by means of a standard Ffowcs Williams and Hawkings (FWH) integral (restricted to the loading noise term as in Curle's theory) starting from the pressure fluctuations on the airfoil surface, or using a porous surface formulation (FWH or Kirchhoff) over a control surface surrounding the airfoil. This done using parallelized Onera

solver MIA (developed by G. Reboul) solving these integral formulations in the frequency domain and restricted here to Curle's expression:

$$\hat{p}\left(\vec{x}_{obs},\omega\right)=\int_{S}\hat{p}\left(\vec{x}_{s},\omega\right)n_{s}\frac{\partial\hat{G}\left(\vec{x}_{obs}\left|\vec{x}_{s},\omega\right.\right)}{\partial x_{s}}dS \tag{2}$$

For convenience, the far-field radiation can be also roughly assessed applying a simple 1/R spreading law correction if the computational domain is large enough to satisfy the far-field conditions.

3 VALIDATIONS ON FLAT PLATE CASE

The methodology has been firstly validated on the flat plate case for which Amiet solution is exact. We consider a flat plate with span length L_{span} = 450 mm and chord length c = 150 mm. The HIT Von-Karman spectrum is defined by T_I = 2.5% and Λ = 6 mm, and the convection flow is assumed to be fully uniform and set equal to 60 m/s. These values are related to FLOCON application described in section 4.

In order to get a reasonable CAA grid size, the computation domain is restricted to a radial strip and periodicity conditions are imposed at each side. Nevertheless, it appears that the suited spanwise extent required to ensure a significant part of the spectrum $\Phi_{ww}\left(k_x,k_y\right)$ related to the most energetic values of k_y (first cut-on oblique gusts) is still demanding heavy mesh size (about 100 Million points), involving quite expensive calculations. As done in [19], a simplification is proposed to avoid this problem. Amiet argued that for a far-field observer in the mid-span plane of an infinite flat-plate (practically when the span to chord ratio is greater or equal to 3), the parallel gusts (k_y = 0) are mainly contributing to the radiated noise. Indeed, it can be shown[4] that the contribution of cut-on oblique gusts are giving rise to balancing terms getting fully cancelled in the mid-span plane for a far-field observer.

Following the above observation, only the parallel gusts can be considered in Eq. (1) when injected in the CAA, if the span to chord ratio assumptions are satisfied. However, a factor $2\pi/L_{\text{span}}$ has to be introduced when calculating the far-field PSD. This factor has to be also included in the CAA in order to get the correct aerodynamic response of the full span airfoil. This is done by setting $\Delta k_y = \frac{2\pi}{L_{span}}$. The incoming synthetic turbulence defined by Eq. (1) is restricted to parallel gusts with a maximum spectrum frequency f_{max} = 5000 Hz and a frequency spacing Δf = 100Hz . The CAA strip is set equal to L_{sim} = 10 mm . Note that in order to take into account for compactness effects, the input data will be duplicated in the spanwise direction over the full span before calculating the FWH integral given by Eq. (2). In addition to standard Amiet solutions derived from far-field approximations, a more rigorous semi-analytical calculation is addressed too, consisting in a FWH integration of the pressure jump over the plate numerically computed using Amiet-based aerodynamic function. Thus, the actual acoustic response including oblique cut-on modes contribution with full compactness effects (no far-field approximations) can be assessed and compared to the CAA prediction. A snapshot of the fluctuating pressure issued from direct CAA computation in the mid-span plane is shown in Fig. 1. The possibility of using the direct acoustic pressure field to estimate the far-field PSD with suited scaling factors has been investigated[3] but absolute levels so obtained are doubtful so that we only focus here on the CAA-FWH approach. A comparison of RMS wall pressure distribution issued from CAA and Amiet-based response is presented in Fig. 2, showing a perfect agreement. Fig. 3 presents

the results for a 90° observer point located in the mid-span plane at 1.2 m and 90° over the airfoil. The computed PSD provided by CAA-FWH (with $k_y = 0$) is closed to Amiet-based solutions obtained with and without including the oblique gusts.

In order to check the numerical response of the plate when impacted by oblique gusts, numerical integrations over the plate surface is now performed using the double sum ($k_y \neq 0$) in Eq. (1). The full span mesh is shown in Fig. 4. The RMS levels of pressure disturbances calculated over the surface are plotted in Fig. 5 (right) and compared to the analytical solution deduced from Amiet theory (Fig. 5, left). The agreement is very good, showing quasi-constant distribution in the spanwise direction, as expected. However, the PSD issued from Curle's formulation (MIA code, Eq. (2)) and shown in Fig. 6 (left) is found to be rather chaotic compared to exact Amiet solution. This is due to cancellation effects between spanwise waves related to the same axial wave number (i.e., same frequency). To reduce these statistical deviations two averaging processes are suggested. The standard one is to perform a quadratic averaging over independent runs. The second one is to realize a smoothing by integrating the spectrum over consecutive frequency bands. Both methods are applied using 10 averages and compared to Amiet solution in Fig. 6, right. The predictions (with only 10 averages) are highly improved more particularly with the second approach which has a practical advantage to prevent from having to perform several computation runs.

4 APPLICATION TO AIRFOIL TREATMENTS

The methodology described in Sec. 2 is now used to try to assess the acoustic performance of a passive treatment studied in the framework of the European project FLOCON[3]. It is applied to the baseline configuration (NACA65-1210 airfoil described in Fig 7, left) and a treated airfoil with leading edge serrations designed by Onera (Fig. 10, left). The tests performed in ISVR anechoic wind tunnel[2] have shown significant broadband noise reductions on a wide frequency range for all studied flows[3]. The airfoils have a 0.15 m chord and a 0.45 m span. The spanwise extent of the CAA domain is set equal to $L\text{sim} = 10\ mm$ (as done previously) and the mean flow is assumed to be fully uniform ($Uo = 60\ m/s$). The synthetic turbulent field injected in the computational domain is the same than in Sec. 3.

4.1 Baseline case

The 3D mesh for the baseline configuration shown in Fig. 7, right. The computation domain (1/45 full span extent) consists in approximately 8.5 millions points and a CPU time of around 120 hours on 256 SGI Altix processors is required to get a fully converged solution. The grid is designed to support acoustic frequencies up to 5 kHz, and the simulation time has to be at least equal to 10 ms to ensure a frequency spacing of 100 Hz. As for the flat plate test case, the extracted unsteady data are duplicated in the spanwise direction to reach the actual 0.45 m span. The figure 8 presents the PSD computed by sAbrinA.v0 + MIA for the baseline configuration and for a 90° observer at 1.2 m over the airfoil (corresponding to a microphone position of ISVR test rig). It is compared to the experiment and to an Amiet solution (already plotted in Fig. 3). Although it is expected to be less confident, the direct CAA solution extrapolated to the far-field using spreading law corrections is plotted too. Despite of a noticeable deviation on the peak level and for low frequencies behind 1 kHz, the agreement is quite satisfactory. As shown by 2D computations[3], a better agreement might be obtained if a more representative convection effects (RANS mean flow solution) was considered in the CAA, since the presence of shear layers tend to increase the attenuation slope of the acoustic spectrum. The OASPL predictions are rather

presented in Fig. 9, showing similar directivity patterns between CAA and Amiet solutions, and rather close to the measurement. The simulation reveals a roughly constant under-estimation around 5 dB over all angles due to the level deviation of low-frequency bump visible in Fig. 8.

4.2 Serrated airfoil response (parallel gusts)

The serrated airfoil calculation requires a finer discretization in the spanwise direction, leading to a mesh with about 13.5 millions grid points. The CPU time is around 300 hours on 256 processors. A partial view of the CAA grid is presented in Fig. 10, right. The 10 mm strip is equal to the wavelength of the serrations (one motif).
Aerodynamic response analyzes are proposed in Figs 11 and 12, related to RMS wall pressure distributions over the airfoil surface (Fig. 11) and along the chord (Fig. 12), for baseline and serration case. The iso-contour map of surface pressure on baseline case (Fig. 11, left) is quite similar to the one of the flat plate case shown in Fig. 5 left. The serration effect is clearly highlighted in Fig. 11 right, revealing a significant reduction of the levels at the top and slopes of the wave. This is addressed more precisely in Fig. 12, showing that pressure profile at the root is close the baseline one, whereas the level is reduced by more than a half at the top and at mid-slope. Significant noise reductions then are expected from these first results.
Fig. 13 shows a PSD comparison between the baseline and the serrated configurations issued from the simulations (Fig. 13 left) and the experiment (Fig. 13 right). Quite similar trends are displayed between the measurements and the numerical predictions with very close level reductions up to 3,5 kHz. This is an excellent result regarding to the complexity of the physics and the rather simplicity of the present method. Beyond, the PWL attenuation due to the serrations is over-estimated by the simulations. It might be due to the fact that oblique gusts ($k_y \neq 0$) contribution, not taken into account here, is no more negligible at these frequencies (contrarily to the straight leading edge case). As a consequence, it could tend to balance the overall level since the spanwise gusts are getting more and more cut-on at higher frequencies. Complementary analysis and discussion about the contribution of oblique gust to the wavy-edge airfoil response are proposed in the next paragraph.

4.3 Response to oblique gusts

As already discussed in [3], a simplified modeling of the present leading edge serrations can be suggested by approximating the sinusoidal geometry by triangular waves (Fig. 14). Thus, it is possible to introduce a lean angle, γ, and to extend the dispersion relation[20] used by Amiet by means of suited variable transformations:

$$k^2 = \left(\frac{\bar{K}_\zeta M}{\beta^2} \right)^2 - \left(\frac{\bar{K}_\zeta M^2}{\beta^2} \tan\gamma + \frac{\bar{K}_\eta}{\beta} \right)^2 \tag{3}$$

Standard dispersion relation is recovered by setting $\gamma = 0°$ in Eq. (3). Roots of second order equation $k^2 = 0$ can be easily obtained allowing us to draw the spatial filtering of axial/spanwise gusts as a function of the lean angle as done in Fig. 15. Indeed, for high values of γ (close to 90 deg.), this representation helps to understand the previous results relative to Fig. 13.
For the baseline case (in red) only oblique gusts with spanwise wavelengths greater than 40 mm should contribute to the radiated noise even up to 10 kHz, which is coherent with Amiet solutions plotted in Fig. 3 and showing slight differences with parallel gust response at high

frequencies (beyond 3 kHz) when the oblique gusts are included. On the other hand, for the serration case, spanwise wavelengths equal to 10 mm are able to be cut-on beyond 3 kHz. As it is equal to the serration wavelength, the serrated airfoil response is expected to be particularly sensitive (resonance effects) to this spanwise frequency and to its harmonics. This might explain the balance of the experimental levels and the limits of the acoustic performance of the serrations in the high-frequency range as observed in Fig. 13 right.

5 CONCLUSIONS

A numerical method aiming to predict the turbulence-airfoil noise and to estimate the acoustic performances of leading edge serrations has been presented and successfully applied in this paper. It is based on a CAA code solving the Disturbance Euler equations and a 2D synthetic turbulence model fitting the turbulence spectrum characteristics prescribed at the inflow of the CAA domain by means of Tam's injection BC. Although an accurate RANS mean flow was available, uniform mean flow assumption has been considered in order to avoid additional difficulties in the convection of turbulent-like velocities. The method has been firstly validated with accuracy on the academic flat-plate case by comparison with exact Amiet solution. Then, it has been used to characterize the acoustic response of a NACA6512-10 airfoil and the effect of wavy leading edges designed by Onera.

The PSD issued from the simulations are found to be in a fairly good agreement with the measurements obtained in ISVR wind tunnel tests. The low-frequency bump observed in the experimental spectrum might be attributed to additional source mechanisms, whereas the deviations observed in the high-frequency range (beyond 4 kHz) for the serrated wing should be due to the spanwise gusts contribution neglected in the CAA. A basic theoretical analysis about spatial filtering of oblique gusts w/ and w/o serrations has been proposed to argue this last point.

Next step will be to perform a complementary computation on the serration case including oblique gusts, requiring for a larger spanwise extent and so leading to a much higher grid size (at least 60 M points) and CPU time. Finally, the present methodology should be adapted and quickly applied to the annular cascade benchmark[21] and then to realistic rotor/stator interaction (broadband) noise problem.

6 ACKNOWLEDGEMENTS

This study has been supported by European Commission (FLOCON FP6 project).

7 REFERENCES

1. M. Jacob, J. Boudet, D. Casalino, M. Michard, "A rod-airfoil experiment as benchmark for broadband noise modeling", *Theoretical and Computational Fluid Dynamics* **19**, pp. 171-196, 2005.
2. M. Gruber, P. Joseph, T. P. Chong, "Experimental investigation of airfoil self noise and turbulent wake reduction by the use of trailing edge serrations", *16th AIAA/CEAS Conference,* 2010-3803, 2010.
3. C. Polacsek, G. Reboul, V. Clair, T. Le Garrec T., H. Deniau, "Turbulence-airfoil interaction noise reduction using wavy leading edge: An experimental and numerical study", *Internoise2011*, Osaka (Japan), 2011.
4. R. K. Amiet, "Acoustic radiation from an airfoil in a turbulent stream", *J. Sound Vib.*, **41**, pp. 407-420, 1975.

5. D. P. Lockard and P. J. Morris, "Radiated noise from airfoils in realistic mean flows", *AIAA Journal* **36(6)**, pp. 907-914, 1998.
6. J. R. Scott, "Single airfoil gust response problem", *4th CAA Workshop on Benchmark Problems*, NASA CP-2004-212954, pp.45-58, 2003.
7. V. V. Golubev, R. R. Mankbadi and J. R. Scott, "Numerical inviscid analysis of nonlinear airfoil response to impinging high-intensity high-frequency gust", *10th AIAA/CEAS Aeroacoustics Conference*, AIAA-2004-3002, 2004.
8. V. V. Golubev, R. R. Mankbadi, M. R. Visbal, J. R. Scott and R. Hixon, "A parametric study of nonlinear gust-airfoil interaction", *12th AIAA/CEAS Aeroacoustics Conference*, AIAA-2006-2426, 2006.
9. R. Hixon, A. Sescu, M. Nallasamy and S. Sawyer, "Prediction of noise from realistic rotor-wake/stator row-interaction using computational aeroacoustics", *15th AIAA/CEAS Aeroacoustics Conference*, AIAA-2009-3339, 2009.
10. R. Hixon, A. Sescu and S. Sawyer, "Vortical gust boundary condition for realistic rotor wake/stator interaction noise prediction using computational aeroacoustics", *J. Sound and Vib.,* **330***, pp. 3801-3817*, 2011.
11. H. M. Atassi, A. A Ali, O. V. Atassi and I. V. Vinogradov, "Scattering of incident disturbances by an annular cascade in a swirling flow", *J. Fluid Mech*., Vol. 499, pp. 111-138, 2004.
12. R. Ewert, "Slat noise trend predictions using CAA with stochastic sound sources from a random particle mesh method (RPM)", *12th AIAA/CEAS Aeroacoustics Conference*, AIAA-2006-2667, 2006.
13. M. Dieste, G. Gabard, "Synthetic turbulence applied to broadband interaction noise", *15th AIAA/CEAS Conference,* AIAA-2009-3267, 2009.
14. A. H. Salem-Said, "Large eddy simulation of shear-free interaction of homogeneous turbulence with a flat-plate cascade", *PhD Thesis*, Virginia Polytechnic Institute and State University, 2007.
15. H. Deniau, G. Dufour, J. F. Boussuge, C. Polacsek, S. Moreau, "Affordable compressible LES of airfoil-turbulence interaction in a free jet", *17th AIAA/CEAS Conference,* AIAA-2011-2707, 2011.
16. S. Redonnet, E. Manoha, P. Sagaut, "Numerical simulations of propagation of small perturbations interacting with flows and solid bodies", *17th AIAA/CEAS Conference,* Paper 2001-222, 2001.
17. C. K. W Tam, "Advances in numerical boundary conditions for computational aeroacoustics", *Journal of Computational Acoustics* **6**, pp. 377-402, 1998.
18. R. H. Kraichnan, "Diffusion by a random velocity field", *Physics of fluids* **13(1)**, pp. 22-31, 1970.
19. J. Casper, F. Farassat, "A new time domain formulation for broadband noise predictions", *International Journal of Aeroacoustics* **1(3)**, pp. 207-240, 2002.
20. J. M. R Graham, "Similarity rules for thin aerofoils in non-stationary subsonic flows," *Journal of Fluid Mechanics* **43(4)**, pp. 753-766, 1970.
21. M. Namba, J. Schulten, "Category 4-Fan Stator with Harmonic Excitation by Rotor Wake", in M. Dahl (Ed.), *Third Computational Aeroacoustics (CAA) Worshop on Benchmark Problems NASA/CP-2000-209790*, pp. 73-86, 2000.

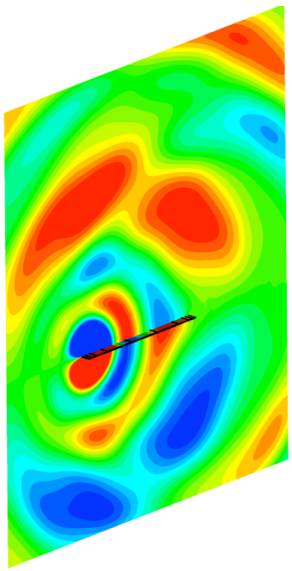


Fig. 1 – Snapshot of disturbance pressure field in the mid-plane

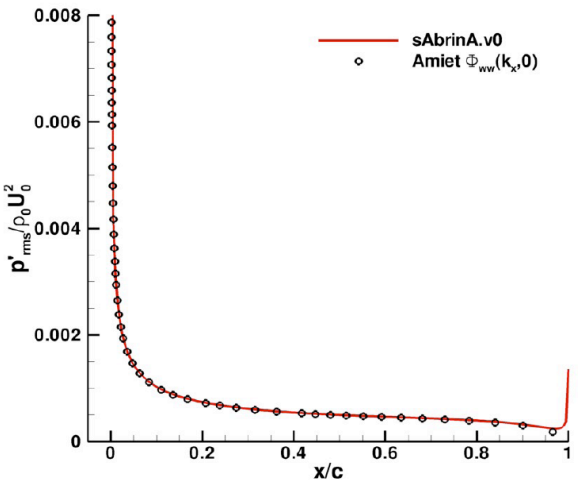


Fig. 2 – RMS wall pressure along the chord

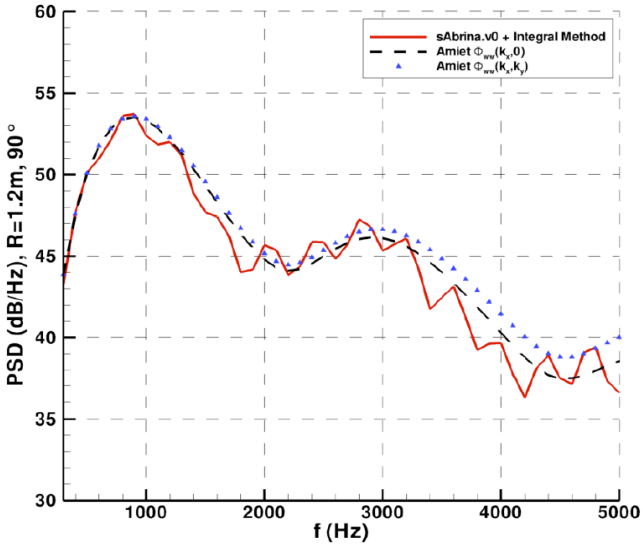


Fig. 3 – Predicted PSD at 90° and R_{obs} = 1.2 m using parallel gusts

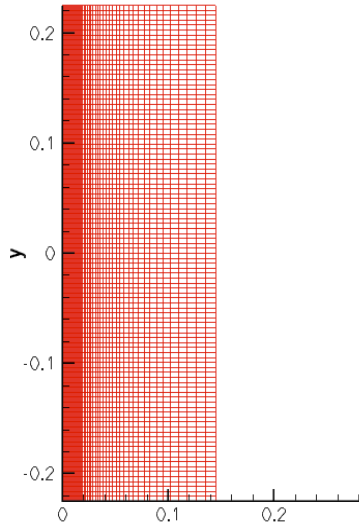


Fig. 4 – Flat plate mesh

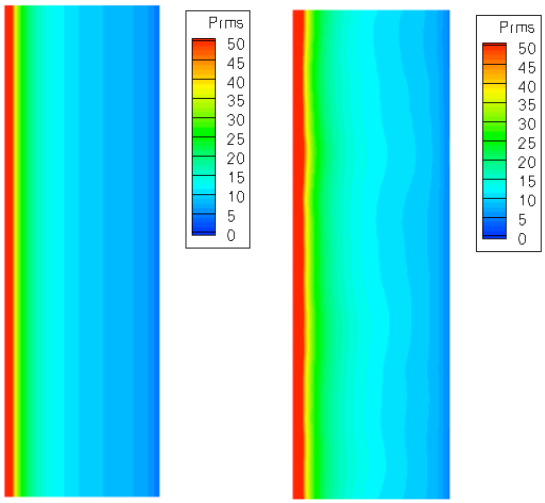


Fig. 5 –RMS surface pressure issued from theory (left) and computation (right)

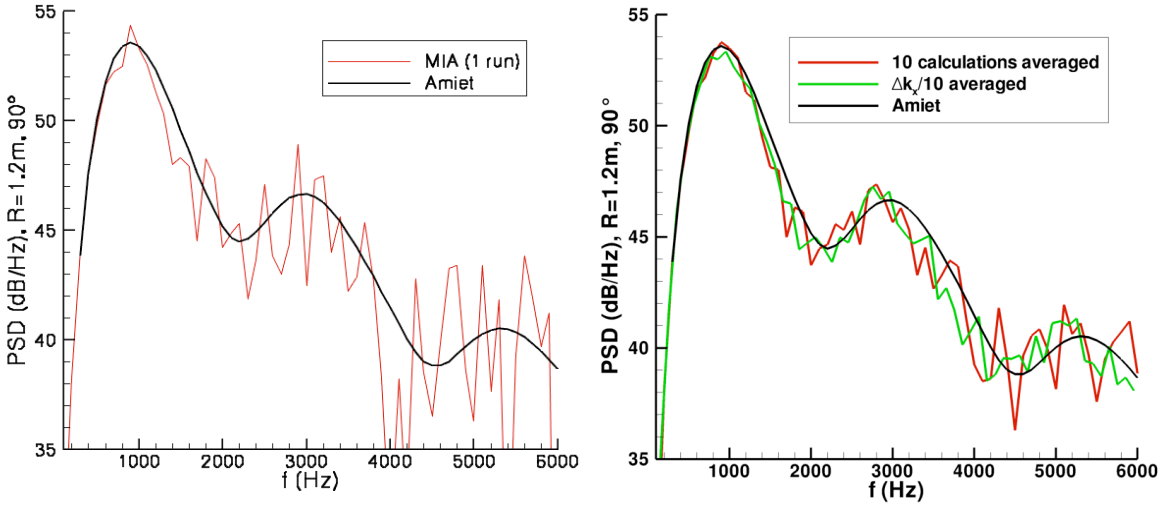


Fig. 6 – Predicted PSD at 90° and R_{obs} = 1.2 m using oblique gusts: without averaging (left) and with averaging over 10 runs (Δf) or over 10 frequency bands of 1 run with Δf/10 (right)

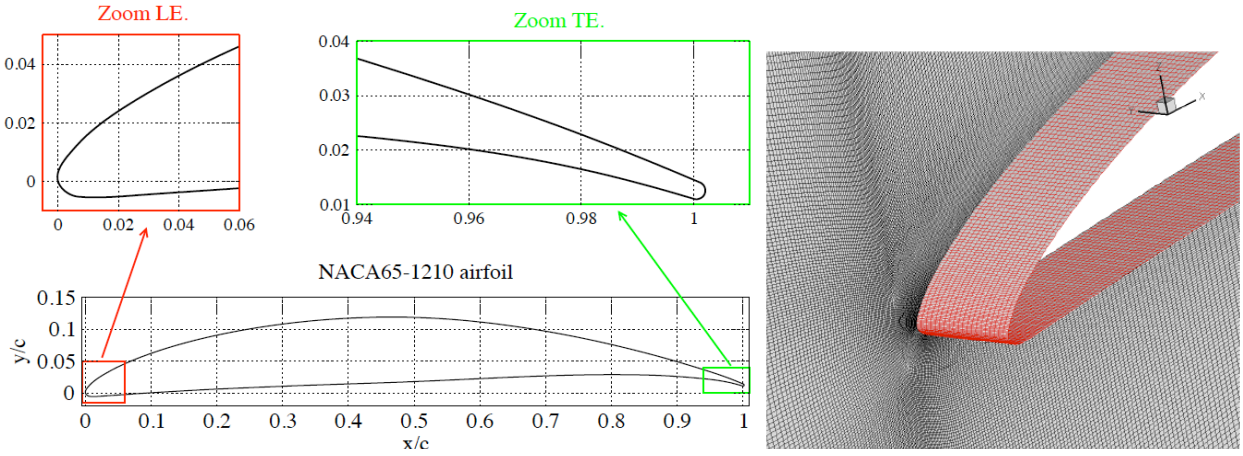
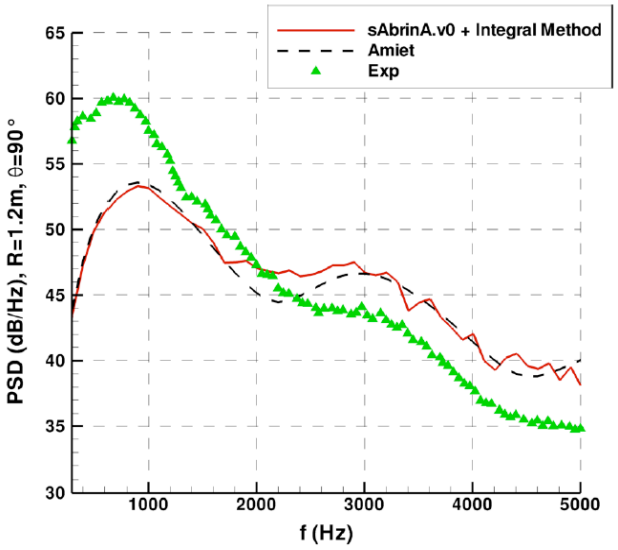


Fig. 7 – NACA6512-10 airfoil geometry (left) and 3D partial view of CAA mesh (right)



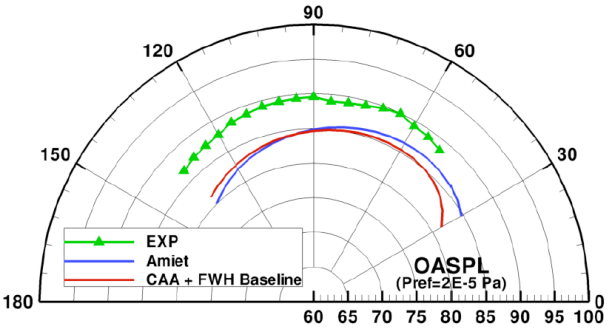


Fig. 8 – PSD (dB/Hz) comparisons at 1.2 m (90°) *Fig. 9 – OASPL (dB) comparisons at 1.2 m*

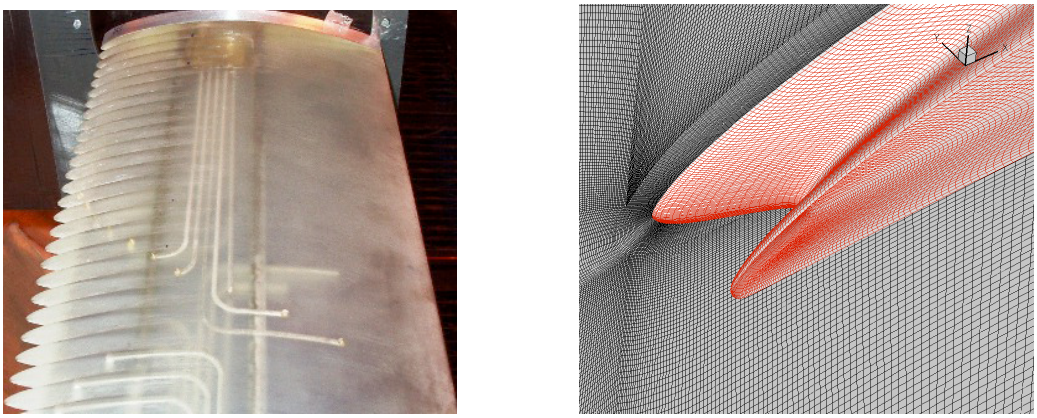


Fig. 10 – Picture of Onera wing (left) and 3D partial view of CAA mesh of serrated wing (right)

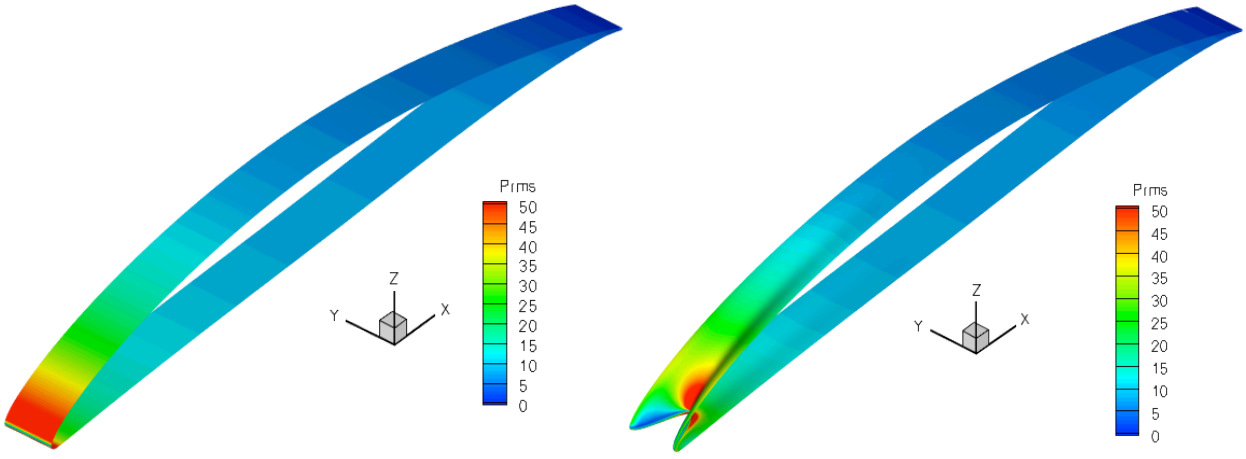


Fig. 11 – RMS surface pressure issued from CAA on baseline (left) and serration case (right)

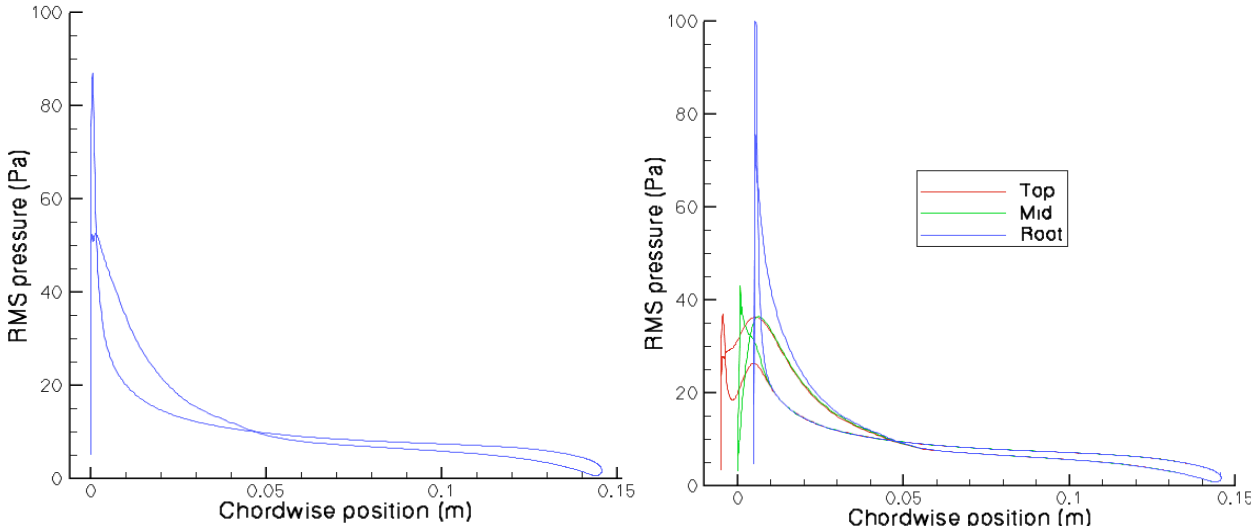


Fig. 12 – CAA chordwise pressure profile (RMS) on baseline (left) and serration case (right)

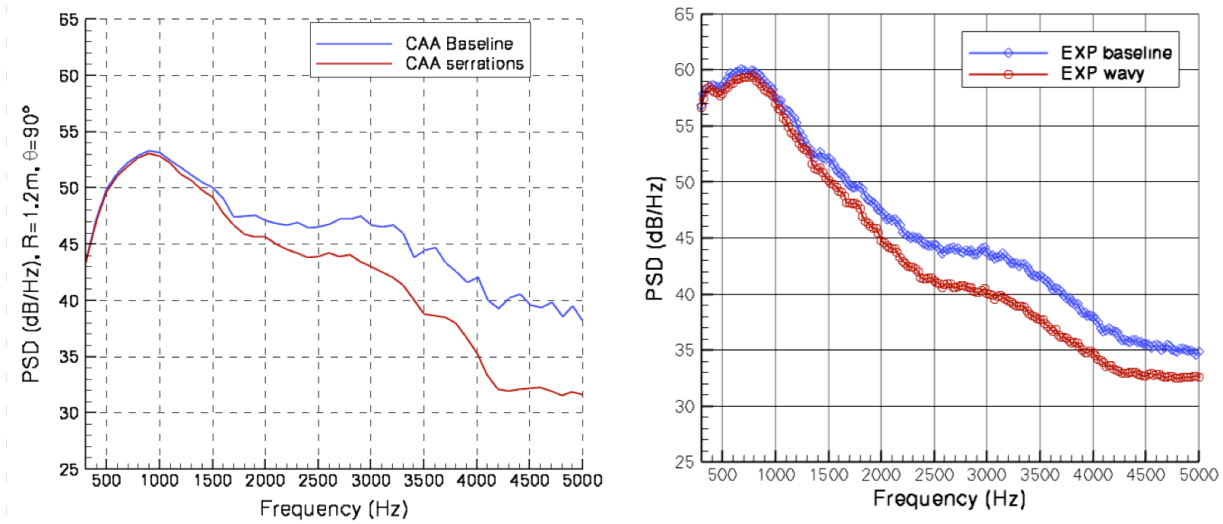


Fig. 13 – PSD comparisons between baseline and serrated airfoils: CAA (left) and experiment (right)

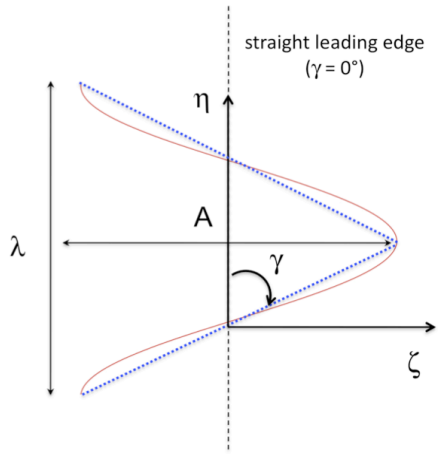


Fig. 14 – Triangular approximation

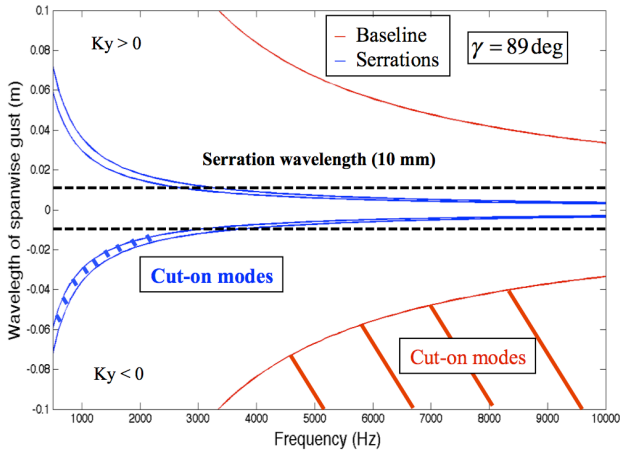


Fig. 15 – Filtering of oblique gusts w/ or w/o serrations